Proc. Natl. Acad. Sci. USA
Vol. 78, No. 6, pp. 3581–3585, June 1981
Biophysics

Resonance Raman investigation of dioxygen bonding in oxycobaltmyoglobin and oxycobalthemoglobin: Structural implication of splittings of the bound O—O stretching vibration

(cobalt-substituted hemoproteins)

MOTONARI TSUBAKI AND NAI-TENG YU†

School of Chemistry, Georgia Institute of Technology, Atlanta, Georgia 30332

Communicated by J. L. Oncley, March 6, 1981

ABSTRACT **Splittings related to the stretching vibration of bound dioxygen in hemoproteins have been detected by resonance Raman spectroscopy. With excitation at 406.7 nm we observe three isotope-sensitive lines in oxycobaltmyoglobin (oxyCoMb) [or in oxycobalthemoglobin A (oxyCoHbA)] at 1103 (1107), 1137 (1137), and 1153 (1152) cm^{-1}, of which the most intense one appears at 1137 cm^{-1}. The first two frequencies arise from resonance interaction between a ν(O—O) mode at ≈1122 cm^{-1} and an accidentally degenerate porphyrin ring mode at 1123 (1121) cm^{-1}, whereas the third one represents an "unperturbed" ν(O—O) vibration from a different species. These two ν(O—O) modes at ≈1122 and ≈1153 cm^{-1} shift to ≈1066 and ≈1096 cm^{-1}, respectively, upon $^{16}O_2 \rightarrow {}^{18}O_2$ substitution. The same resonance interaction may also occur in oxyFeMb (probably also in oxyFeHbA), because it exhibits an intensity increase at 1125 cm^{-1} upon $^{16}O_2 \rightarrow {}^{18}O_2$ substitution, although the ν(O—O) vibrations have not been observed directly. Concomitant enhancement is observed in the ν(Co—O) vibration at 539 (537) cm^{-1}, which is considerably lower than the ν(Fe—O) frequency at ≈570 cm^{-1} in oxyFeMb and oxyFeHbA. The Co—O bond is longer and weaker than the Fe—O bond. Enhancement of both ν(O—O) and ν(Co—O) indicates the existence of a charge-transfer transition underlying the Soret band, which may be assigned as $\pi^*(\pi_g^*O_2/d_{xz}) \rightarrow \sigma^*(d_{z^2}Co/\pi_g^*)$. The presence of two ν(O—O) vibrations (at ≈1122 and ≈1152 cm^{-1}) but only one ν(Co—O) mode (at ≈538 cm^{-1}) means that the two species in oxyCoMb or oxyCoHbA have the same Co—O bond lengths but different O—O bond lengths. The bound dioxygen in a bent end-on configuration may have two allowed orientations, which differ in the extent of $sp^2(N_\epsilon) \rightarrow \pi^*(O_2)$ donation from distal histidine.**

The nature of bound dioxygen in oxyhemoglobin (oxyHb) and oxymyoglobin (oxyMb) has been the subject of numerous experimental studies and speculations (1–7). One of the most useful "fingerprint" properties of coordinated O_2 is the vibrational spectrum of the Fe—O_2 moiety—i.e., the frequencies of ν(O—O) and ν(Fe—O) stretching vibrations. The ν(O—O) frequencies at 1107 (oxyHbA) and 1103 cm^{-1} (oxyMb) were reported by Caughey and coworkers (8, 9), who employed infrared difference spectroscopy. Subsequent work (10) on cobalt-substituted oxyhemoglobin A (oxyCoHbA) (containing Co-deuteroporphyrin IX) revealed a very similar ν(O—O) vibration at 1105 cm^{-1} for Co-bound O_2. These values, being close to those of free superoxide ions (1100–1150 cm^{-1}), have been taken as evidence of a substantial transfer of electron density from the iron (or cobalt) to the coordinated oxygen. The charge-transfer formulation of Fe(III)—O_2^- or Co (III)—O_2^- has, in fact, been proposed by many investigators (2, 5, 7, 11–14), although there is not necessarily a transfer of an electron from Fe (or Co) to O_2 upon binding (4, 15, 16). The picture of single ν(O—O) vibration is complicated by the discovery of an additional infrared band at 1156 cm^{-1} in oxyHbA (17) after Collman *et al.* (13) reported the ν(O—O) mode at ≈1150–1160 cm^{-1} in the oxygen adducts of Fe and Co "picket fence" porphyrins. The splitting of ν(O—O) mode into two infrared bands of comparable intensity at 1107 and 1156 cm^{-1} in oxyHbA was interpreted (17) as due to Fermi resonance with the first overtone of ν(Fe—O) stretch at ≈570 cm^{-1} (originally reported at 567 cm^{-1}) observed by Brunner (18), using resonance Raman spectroscopy. On the basis of this interpretation, one would predict the existence of an infrared ν(O—O) band at ≈ 1156 cm^{-1} in oxyCoHbA and the consequence of Fermi resonance would place the ν(Co—O) stretching frequency at ≈570 cm^{-1}.

In view of the importance of ν(O—O) vibration in understanding the exact nature of dioxygen bonding in oxyHb and oxyMb, we decided to carry out resonance Raman studies of cobalt-substituted oxyHbA and oxyMb with a view toward the possibility of observing both ν(O—O) and ν(Co—O) vibrations.‡ Raman spectroscopy is capable of detecting these two vibrations via resonance enhancement with a charge-transfer transition involving the π electron of O_2 and the molecular orbitals that would affect the Co—O bond length upon electron promotion. However, no resonance Raman detection of ν(O—O) from bound dioxygen in hemoproteins has been reported to date.

In this paper, we report the observation of both ν(O—O) and ν(Co—O) in oxyCoHbA and oxyCoMb upon excitation at 406.7 nm. Three lines near 1100 cm^{-1} sensitive to $^{16}O_2 \rightarrow {}^{18}O_2$ substitution have been identified at ≈1107, ≈1137, and ≈1152 cm^{-1}. We will show that the frequency at 1107 cm^{-1} is not a "genuine" ν(O—O) stretching vibration; instead it is a "perturbed" porphyrin ring mode mixed with some ν(O—O) characters. In essence, there are two independent ν(O—O) vibrations at ≈1122 and ≈1152 cm^{-1} representing two different species. The first ν(O—O) at ≈1122 cm^{-1} then undergoes a vibrational perturbation (resonance interaction) with one of the porphyrin ring modes, giving rise to two split lines at ≈1107 and ≈1137 cm^{-1}. We have not observed directly the corre-

The publication costs of this article were defrayed in part by page charge payment. This article must therefore be hereby marked "*advertisement*" in accordance with 18 U. S. C. §1734 solely to indicate this fact.

Abbreviations: CoHb and CoMb, cobalt-substituted hemoglobin and myoglobin, respectively (FeHb and FeMb indicate the natural iron hemoproteins); meso- and deutero-, mesoporphyrin IX- and deuteroporphyrin IX-substituted hemoproteins.

† To whom reprint requests should be addressed.

‡ Resonance Raman enhancement of ν(O—O), but not ν(Co—O), in a macrocyclic Co(II) complex was reported previously by Szymanski *et al.* (19).

sponding ν(O—O) vibrations in oxyFeHbA and oxyFeMb, but the intensity increase at 1125 cm^{-1} in oxyFeMb upon $^{16}O_2 \rightarrow {}^{18}O_2$ substitution indicates that the same resonance interaction may also be operative in Fe hemes.

Because cobalt-substituted hemoglobin and myoglobin mimic the native hemoproteins in biological functions, including the cooperative oxygen binding of CoHb, we believe that results from oxyCoHbA and oxyCoMb should have a direct bearing on dioxygen bonding in native oxyHb and oxyMb.

MATERIALS AND METHODS

Sperm whale myoglobin was purchased from Sigma and further purified as described (20). The purified metmyoglobin was then reduced by sodium dithionite anaerobically, followed by anaerobic gel filtration in 0.01 M sodium phosphate buffer, pH 6.9 (2.26 g of $NaH_2PO_4 \cdot 2H_2O$ and 2.52 g of Na_2HPO_4 per 5 liters), and exposure to the air to form oxyMb. For further purification, oxyMb solution was applied to a column of CM-52 carboxymethyl-cellulose (Whatman) equilibrated with 0.01 M sodium phosphate buffer, pH 6.9. After washing with the same buffer, the weakly adsorbed oxyMb was slowly eluted by 0.02 M sodium phosphate buffer, pH 7.2 (0.80 g of $NaH_2PO_4 \cdot 2H_2O$ and 1.05 g of Na_2HPO_4 per liter).

Human hemoglobin A was prepared in oxy form by the usual procedure, starting from whole blood (21).

The heme group was removed from metmyoglobin or methemoglobin A by the method of Teale (22), using 2-butanone. The incorporation of cobalt protoporphyrin IX into apoproteins was carried out by the method of Yonetani *et al.* (23). The procedure of Tsubaki and Nagai (24) was used for the purification of oxyCoHbA. For purifying oxyCoMb we employed the same procedure described above for oxyMb. Oxy cobalt α and β globin chains were prepared according to the method of Tsubaki and Nagai (24).

The heme concentration was determined spectrophotometrically in oxygenated form for iron derivatives and in deoxygenated form for cobalt derivatives. The extinction coefficients used are 14.6 mM^{-1} cm^{-1} at 577 nm (oxyFeHbA), 14.6 mM^{-1} cm^{-1} at 581 nm (oxyFeMb), 17.0 mM^{-1} cm^{-1} at 552 nm (deoxyCoHbA), and 17.0 mM^{-1} cm^{-1} at 558 nm (deoxyCoMb).

Raman spectra were obtained by using a highly sensitive multichannel Raman system, which has been described in detail elsewhere (25). The spectrometer consists of two 600 grooves per mm classically ruled gratings in additive dispersion, which has been demonstrated (20, 26) to be well suited for resonance Raman spectroscopy of heme proteins. The 500-channel intensified vidicon detector (a Princeton Applied Research dry ice-cooled SIT model 1254/01) can view an approximately 600-cm^{-1} segment of a Raman spectrum excited at ≈400 nm. Large dynamic range and the capability for long-term data integration, which minimizes the preamplifier noises, make it an ideal device for extracting extremely weak Raman signals from the background. Its enhanced detection capability over a conventional photomultiplier-photon counting system allows us to obtain high-quality resonance Raman spectra of oxyCoMb and oxyCoHbA without detectable photodissociation. The average laser power used to obtain the spectra in the present study is ≈15 mW or less.

The major exciting wavelength at 406.7 nm was provided by a Spectra-Physics model 171-01 krypton ion laser. Other lasers used were: Coherent Radiation CR-8 (Ar^+) and CR-500 (Kr^+). A 90° scattering geometry was used, and the sample rotating cell was kept spinning during the measurements to avoid local heating and partial photodissociation of bound dioxygen. All Raman spectra presented here have not been computer-smoothed.

For $^{18}O_2$ isotope substitution experiments, the sample solution was deoxygenated in the rubber sealer rotating quartz cell by repeated evacuation and flushing with pure nitrogen gas. After the final evacuation, the $^{18}O_2$ gas (99 atom %, Stohler Isotope Chemicals) was introduced at an initial pressure of 1 atmosphere.

RESULTS

Resonance Raman spectra in the 100- to 700-cm^{-1} region of oxyCoMb and oxyCoHbA are presented in Fig. 1. Upon substitution of $^{16}O_2$ by $^{18}O_2$, two lines at 539 (oxyCoMb) and 537 cm^{-1} (oxyCoHbA) were shifted to 516 and 514 cm^{-1}, respectively. These lines are assigned to the cobalt–oxygen stretching vibration ν(Co—O). The 23-cm^{-1} shift is very close to the value (22 cm^{-1}) calculated on the basis of the model imidazole—Co—O—O with the Co—O—O angle = 130° (27). The ν(Co—O) value at ≈538 cm^{-1} is considerably lower than that of ν(Fe—O) at 573 (oxyFeMb) or 570 cm^{-1} (oxyFeHbA).§ Because the Co—O—O and Fe—O—O moieties have similar geometries (27, 30), the 34-cm^{-1} difference between ν(Fe—O) and ν(Co—O) cannot be accounted for by different degrees of mixing in the normal mode or by the mass effect, which would shift the frequency by ≈4 cm^{-1}. Thus, the additional shift of ≈30 cm^{-1} must be attributed to the weakening of the Co—O bond relative to the Fe—O bond. The weaker bond between cobalt and oxygen was suggested by the equilibrium measurements of dioxygen binding to CoHbA and CoMb (23) and also by temperature-jump kinetic studies, which showed that the

§ The cited values are from our own measurements. The ν(Fe—O) frequency was reported by Brunner (18) at 567 cm^{-1} in oxyFeHbA, as compared to 572 cm^{-1} by Nagai *et al.* (28) and Duff *et al.* (29).

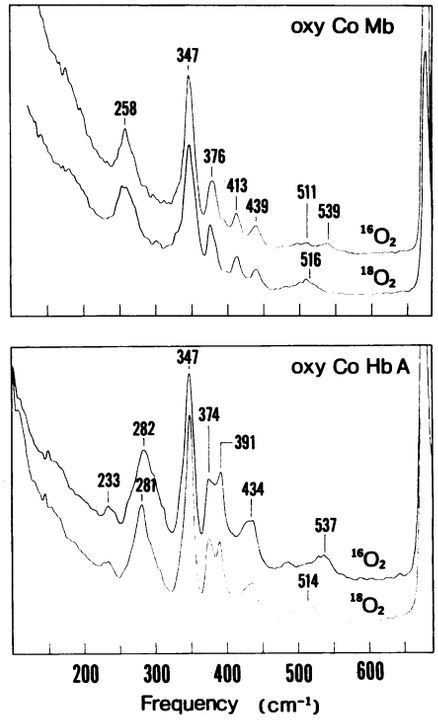

FIG. 1. Resonance Raman spectra of oxyCoMb (*Upper*) and oxyCoHbA (*Lower*) in the 100- to 700-cm^{-1} region. Conditions: excitation wavelength 406.7 nm; laser power, 15 mW at sample; slit width, 100 μm; data integration time, 303 sec (10,000 delay cycles, 100 readout scans); protein concentration 40–50 μM (heme basis) in 0.05 M Tris·HCl buffer, pH 8.3.

dissociation rate constants (k_{off}) for Co hemoproteins are $\approx 10^2$ times larger than those for Fe derivatives, whereas the association rate constants (k_{on}) are in the same order of magnitude for both Co and Fe systems (31).

In Fig. 2 *Upper* we show the resonance Raman spectra of $CoMb^{16}O_2$ and $CoMb^{18}O_2$ in the 900- to 1300-cm^{-1} region, where the ν(O—O) vibrations are expected to appear. The difference spectrum ($^{16}O_2$ minus $^{18}O_2$) shown in Fig. 2 *Lower* was obtained by normalizing the 1229-cm^{-1} line (a porphyrin ring mode) to the same intensity. We were surprised to find that the most prominent line, at 1137 cm^{-1}, does not correspond to any infrared ν(O—O) frequencies in either Co or Fe hemoproteins reported so far. The spectral changes are more clearly seen in the difference spectrum; there it exhibits three positive peaks at $\approx$1103, $\approx$1137, and $\approx$1153 cm^{-1} (as a shoulder) and three negative peaks at 1069, 1096, and 1123 cm^{-1}. To make sure that the observed spectral changes are not due to oxidation or denaturation during repeated evacuation or laser irradiation, we have demonstrated that after exposing the $CoMb^{18}O_2$ sample to oxygen gas ($^{16}O_2$) for 30 min we were able to recover completely the $CoMb^{16}O_2$ spectrum, which is also shown in Fig. 2 *Upper* (third curve). It should be noted that the sum of the integrated intensities of positive peaks is not equal to that of negative peaks.

Fig. 3 shows more clearly the presence of a positive peak at 1152 cm^{-1} in the case of oxyCoHbA. The peaks at 1107 (positive) and 1095 cm^{-1} (negative) are also more pronounced than the corresponding ones in oxyCoMb (Fig. 2). When protoporphyrin IX is replaced by mesoporphyrin IX, the difference spectrum ($^{16}O_2$ minus $^{18}O_2$) of oxyCo-meso-Mb exhibits the absence of the peaks at 1152 and 1095 cm^{-1} (unpublished results).

Unlike the cobalt derivatives, the native iron-containing oxyHbA and oxyMb exhibit no lines that can be shifted to lower frequencies by $^{16}O_2 \rightarrow {}^{18}O_2$ replacement. Instead we observed

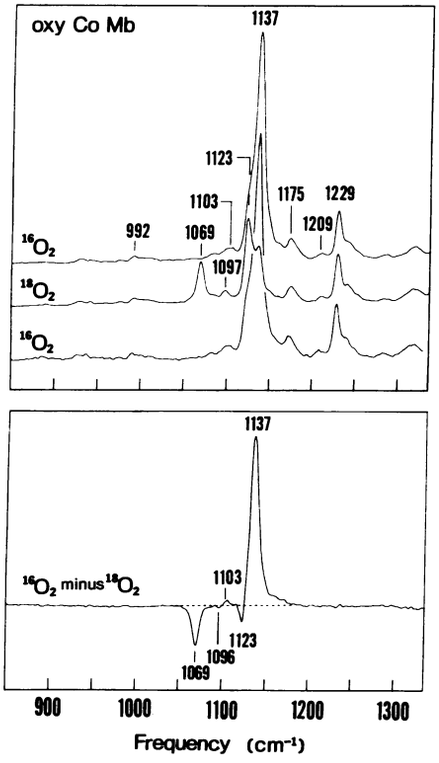

FIG. 2. Resonance Raman spectra of oxyCoMb (*Upper*) and difference spectrum ($CoMb^{16}O_2$ minus $CoMb^{18}O_2$) (*Lower*) in the 900- to 1300-cm^{-1} region. Experimental conditions are the same as for Fig. 1.

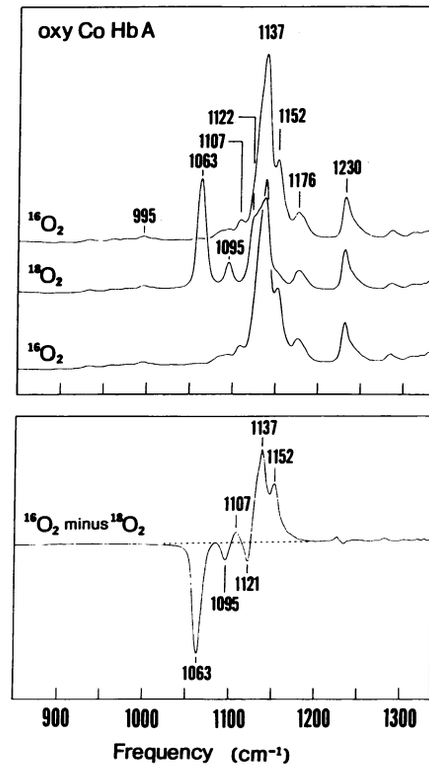

FIG. 3. Resonance Raman spectra of oxyCoHbA (*Upper*) and difference spectrum ($CoHbA^{16}O_2$ minus $CoHbA^{18}O_2$) (*Lower*) in the 900- to 1300-cm^{-1} region.

a definite and clear intensity increase at 1125 cm^{-1} in the $^{18}O_2$ spectrum (Fig. 4). Again, this increase of intensity at 1125 cm^{-1} is not an artifact, as demonstrated by a complete recovery of the $FeMb^{16}O_2$ spectrum (third curve of Fig. 4 *Upper*) after the exposure of the $FeMb^{18}O_2$ sample to oxygen gas ($^{16}O_2$). However, the intensity increase near 1125 cm^{-1} expected for oxyFeHbA is not very obvious (see Fig. 4 *Lower*).

Resonance Raman spectra (900–1300 cm^{-1}) of isolated oxyCo α and β chains are displayed in Fig. 5, which shows a stronger 1152-cm^{-1} peak for the β chain. The positions of positive and negative peaks are very similar to those in oxyCoHbA (Fig. 3). The peak at 1152 cm^{-1} in the spectrum of oxyCoHbA appears to derive mostly from the β subunit. In contrast to the oxyCoMb and oxyCo α cases, the total integrated intensity of positive peaks in oxyCoHbA and oxyCo β is approximately equal to that of negative peaks.

In addition, we found that the spectral features observed near 1100 cm^{-1} in oxyCoMb did not change with pH variations between 6.0 and 10.0.

DISCUSSION

Splittings of O—O Stretching Frequency. A total of six Raman lines near 1100 cm^{-1} are candidates for the assignment of ^{16}O—^{16}O and ^{18}O—^{18}O stretching vibrations. The first three lines are located at *1103 (1107)*, 1137 (1137), and *$\approx$1153 (1152)* cm^{-1} in the spectrum of $CoMb^{16}O_2$ (or $CoHb^{16}O_2$); and the remaining three are at *1069 (1063)*, 1096 (1095), and 1123 (1121) cm^{-1} in $CoMb^{18}O_2$ (or $CoHb^{18}O_2$). The italicized frequencies are very similar to and thus presumably correspond to the infrared bands reported at: 1105 [Co-deutero-$Hb^{16}O_2$ (deutero-indicating substitution by deuteroporphyrin IX)], 1107 ($FeHb^{16}O_2$), 1103 ($FeMb^{16}O_2$), 1065 (Co-deutero-$Hb^{18}O_2$), 1066 ($FeHb^{18}O_2$ and $FeMb^{18}O_2$), and 1156 cm^{-1} ($FeHb^{16}O_2$) (8–10, 17).

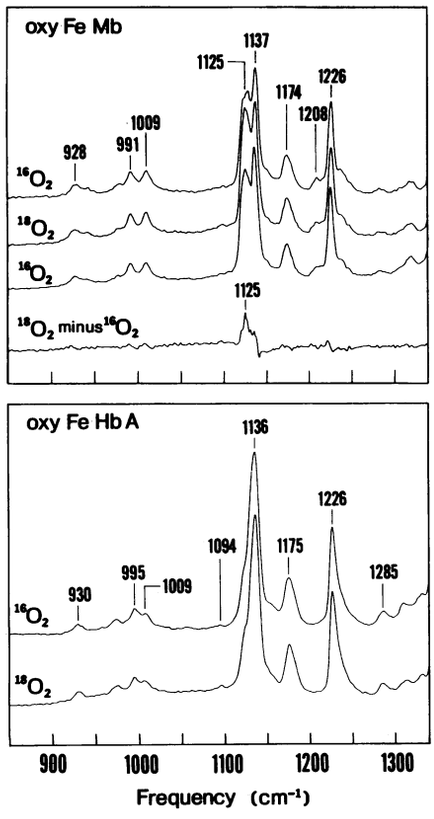

FIG. 4. Resonance Raman spectra of oxyFeMb (*Upper*) and oxyFeHbA (*Lower*). Experimental conditions are the same as for Fig. 1.

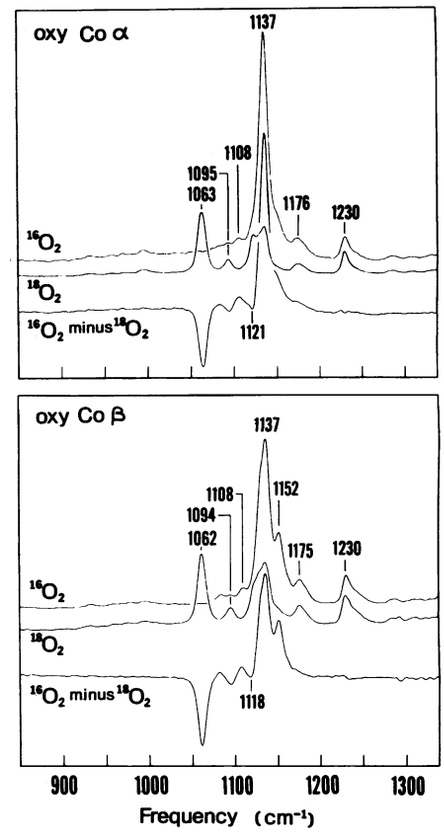

FIG. 5. Resonance Raman spectra of oxyCo α chain and difference spectrum (Co α $^{16}O_2$ minus Co α $^{18}O_2$) (*Upper*). Resonance Raman spectra of oxyCo β chain and difference spectrum (Co β $^{16}O_2$ minus Co β $^{18}O_2$) (*Lower*). Experimental conditions are the same as for Fig. 1.

Analysis of our data reveals a number of important clues: (*i*) The mean of 1103 (1107) and 1137 (1137) is very close to 1123 (1121) cm^{-1}. (*ii*) The intensities at ≈1153 (1152) for $^{16}O_2$ and at 1096 (1095) cm^{-1} for $^{18}O_2$ appear to increase or decrease together and in one instance we have observed the complete disappearance of both lines in the difference spectrum between Co-meso-Mb$^{16}O_2$ and Co-meso-Mb$^{18}O_2$ (unpublished results). (*iii*) The ratios 1152/1095 and 1122/1066 are both 1.05 expected for metal-bound O—O stretch. (*iv*) The first overtone of Co—O stretch (i.e., 2 × 538 cm^{-1}) is 53 cm^{-1} less than the mean of 1103 (1107) and 1153 (1152) cm^{-1}. This information has led us to propose that: (*i*) There exist two species having different O—O bond lengths (hence force constants) that give rise to two independent ν(O—O) frequencies at ≈1122 and ≈1152 cm^{-1}. (*ii*) The ν(O—O) mode at ≈1122 cm^{-1} has suffered a vibrational perturbation (resonance interaction) with an accidentally degenerate porphyrin ring mode, resulting in two frequencies at 1103 (1107) and 1137 (1137) cm^{-1}. (*iii*) Upon $^{18}O_2$ substitution, the aforementioned resonance interaction becomes decoupled and the frequencies at ≈1066 and ≈1095 cm^{-1} may be assigned to ^{18}O—^{18}O vibrations, corresponding to two different species in $^{18}O_2$-substituted hemoproteins. (*iv*) The increase in intensity at ≈1122 cm^{-1} upon $^{16}O_2 \rightarrow {}^{18}O_2$ substitution is clear evidence for the reappearance of the porphyrin ring mode after decoupling because of the mismatch with ν(^{18}O—^{18}O) frequencies. (*v*) The same resonance interaction may also be operative in Fe hemes, because an intensity increase at 1125 cm^{-1} in the spectrum of oxyFeMbO_2 upon $^{18}O_2$ substitution has been clearly observed (Fig. 4).

Structural Implication of Two ν(O—O) Frequencies. The intensity increase observed in oxyFeMbO_2 (Fig. 4) suggests that oxyMb has a ν(O—O) vibration at ≈1125 cm^{-1}. The existence of a second ν(O—O) mode is suggested by the observation of Alben *et al.* (17), who reported an infrared ν(O—O) frequency at 1156 cm^{-1} in oxyFeHbA. The possible origin of two ν(O—O) frequencies in both Fe and Co hemoproteins is provided by a recent high-resolution (at 1.6 Å) x-ray crystallographic study of sperm whale oxyMb (30), which reveals two alternative positions for the terminal oxygen, related by a 40° rotation. With the iron-bound oxygen atom in close contact with the N_ϵ of distal histidine (E7) the rotation of terminal oxygen from the major position may significantly weaken the $sp^2(N_\epsilon)$ donation to the antibonding π^* orbital of O_2, which causes the ν(O—O) frequency to increase. The observed secondary ν(O—O) mode at ≈1152 cm^{-1} is close to the modes of dioxygen adducts of Fe or Co "picket fence" porphyrin complexes (≈1150–1160 cm^{-1}) (13) in which there is no donation to bound dioxygen from the distal site.

The $sp^2(N_\epsilon) \rightarrow \pi^*(O_2)$ donation is expected to affect the $d\pi \rightarrow \pi^*(O_2)$ interaction as well. However, the observation of a single ν(Co—O) or ν(Fe—O) stretching frequency suggests that it may be a second-order effect.

The interaction between the sp^2 orbital of the N_ϵ atom of distal histidine (E7) and the π^* antibonding orbital of bound CO has been proposed in the interpretation of multiple C—O stretching frequencies in carbonmonoxyMb (32) or carbonmonoxy derivatives of abnormal hemoglobins such as Hb Zürich and Hb Emory (33, 34).

In essence, we assign the ν(O—O) mode at 1122 cm^{-1} to a major oxyheme conformer and that at ≈1152 cm^{-1} to a minor one.

Nature of O_2 Bonding and the Charge-Transfer Transition near 400 nm. The bonding between Co (or Fe) and dioxygen arises primarily from the overlap of one of the two dioxygen π_g^*

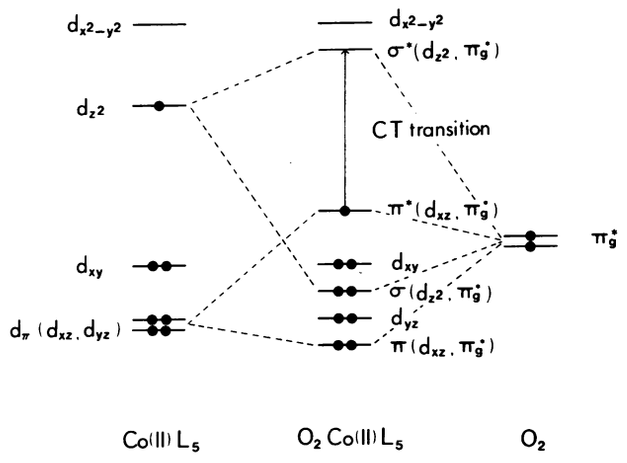

FIG. 6. Simplified energy level diagram for molecular orbitals in the $O_2Co(II)L_5$ system. Actually both d_{xz} and d_{yz} orbitals may share the mixing with $\pi_g^*(O_2)$ orbital, and therefore our arbitrary assignment of the overlap to only d_{xz} is a simplification. CT transition, charge-transfer transition.

orbitals with the d_{z^2} orbital of metal because the O—O axis is considerably tilted from the z axis in a bent end-on configuration. On the other hand, the π interaction between $d_\pi(d_{xz}, d_{yz})$ orbitals and the other $\pi_g^*(O_2)$ orbital may also contribute significantly to the metal–oxygen bond strength. A simplified molecular orbital energy diagram is shown in Fig. 6.

With Co(II) as the metal, there are nine electrons to populate these orbitals; the $\pi^*(d_{xz}/\pi_g^*)$ antibonding orbital is half occupied ($S = \frac{1}{2}$). Electron spin resonance studies (35–37) indicate that the unpaired electron resides in an orbital predominantly localized on dioxygen. In contrast, the bonding $\pi(d_{xz}/\pi_g^*)$ electrons may be localized in Co. With Fe(II) there are eight electrons to fill the orbitals; this leaves the $\pi^*(d_{xz}/\pi_g^*)$ antibonding orbital vacant. Because of the lower nuclear charge of Fe(II) compared to Co(II), the metal d orbitals are slightly stretched and raised in energy. This along with the vacancy in the π^* (d_{xz}/π_g^*) orbital would make a stronger π bonding in Fe hemes.

The Co—O stretching vibration at $\approx$538 cm^{-1}, compared to the Fe—O stretch at $\approx$570 cm^{-1}, may be indicative of a weaker π bonding in the Co—O_2 moiety. However, the frequency at $\approx$538 cm^{-1} is still much higher than the frequencies of Fe(III)—N_3^- (at $\approx$411 cm^{-1}) (26) and Fe(III)—CN^- (at $\approx$455 cm^{-1}) (unpublished results) in hemoglobin derivatives, which may be indicative of synergistic σ and π bondings in Fe—O_2 and Co—O_2 because N_3^- and CN^- are known to be coordinated to Fe(III) almost entirely by σ bonding (38).

Considering the enhancement of both ν(O—O) and ν(Co—O) vibrations in oxy Co hemes, but not in oxy Fe hemes, we propose that the responsible charge-transfer transition involves an electronic promotion from $\pi^*(\pi_g^*/d_{xz})$ to $\sigma^*(d_{z^2}/\pi_g^*)$ (see Fig. 6). This electron displacement should cause elongation of the Co—O bond and contraction of the O—O bond in the excited state, which should be effective in shifting the origin of the potential energy curve along these coordinates. We believe that the Franck–Condon scattering mechanism (39) has contributed significantly to the observed ν(Co—O) and ν(O—O) intensities. In addition, Herzberg–Teller vibronic couplings (39) may also contribute because of the close proximity of the Soret band to the charge-transfer state and its large extinction coefficient.

This research is supported by National Institutes of Health Grant GM 18894. N.-T.Y. is the recipient of National Institutes of Health Research Career Development Award EY 00073, 1976–1981.

1. Pauling, L. & Coryell, C. (1936) *Proc. Natl. Acad. Sci. USA* **22**, 210–216.
2. Weiss, J. J. (1964) *Nature (London)* **202**, 83–84.
3. Griffith, J. S. (1956) *Proc. R. Soc. London Ser. A* **235**, 23–36.
4. Kirchner, R. F. & Loew, G. H. (1977) *J. Am. Chem. Soc.* **99**, 4639–4647.
5. Cerdonio, M., Congiu-Castellano, A., Moguo, F., Pispisa, B., Romani, G. L. & Vitale, S. (1977) *Proc. Natl. Acad. Sci. USA* **74**, 398–400.
6. Eicher, H. & Trautwein, J. (1969) *J. Chem. Phys.* **50**, 2540–2551.
7. Yamamoto, T., Palmer, G., Gill, D., Salmeen, I. T. & Rimai, L. (1973) *J. Biol. Chem.* **248**, 5211–5213.
8. Barlow, C. H., Maxwell, J. C., Wallace, W. J. & Caughey, W. S. (1973) *Biochem. Biophys. Res. Commun.* **55**, 91–95.
9. Maxwell, J. C., Volpe, J. A., Barlow, C. H. & Caughey, W. S. (1974) *Biochem. Biophys. Res. Commun.* **58**, 166–171.
10. Maxwell, J. C. & Caughey, W. S. (1974) *Biochem Biophys. Res. Commun.* **60**, 1309–1314.
11. Lang, G. & Marshall, W. (1966) *Proc. Phys. Soc. (London)* **87**, 3–34.
12. Wittenberg, J. B., Wittenberg, B. A., Peisach, J. & Blumberg, W. E. (1970) *Proc. Natl. Acad. Sci. USA* **67**, 1846–1853.
13. Collman, J. P., Brauman, J. I., Halbert, T. R. & Suslick, K. S. (1976) *Proc. Natl. Acad. Sci. USA* **73**, 3333–3337.
14. Reed, C. A. & Cheung, S. K. (1977) *Proc. Natl. Acad. Sci. USA* **74**, 1780–1784.
15. Tovrog, B. S., Kitko, D. J. & Drago, R. S. (1976) *J. Am. Chem. Soc.* **98**, 5144–5153.
16. Churg, A. K. & Makinen, M. W. (1978) *J. Chem. Phys.* **68**, 1913–1925.
17. Alben, J. O., Bare, G. H. & Moh, P. P. (1978) in *Biochemical and Clinical Aspects of Hemoglobin Abnormalities*, ed. Caughey, W. S. (Academic, New York), pp. 607–617.
18. Brunner, H. (1974) *Naturwissenschaften* **61**, 129.
19. Szymanski, T., Cape, T. W., Van Duyne, R. P. & Basolo, F. (1979) *J. Chem. Soc. Chem. Commun.*, 5–6.
20. Yu, N.-T. & Tsubaki, M. (1980) *Biochemistry* **19**, 4647–4653.
21. Kilmartin, J. V., Hewitt, J. A. & Wooton, J. F. (1975) *J. Mol. Biol.* **93**, 203–218.
22. Teale, F. W. J. (1959) *Biochim. Biophys. Acta* **35**, 543.
23. Yonetani, T., Yamamoto, H. & Woodrow, G. V. (1974) *J. Biol. Chem.* **249**, 682–690.
24. Tsubaki, M. & Nagai, K. (1979) *J. Biochem. (Tokyo)* **86**, 1029–1035.
25. Yu, N.-T. & Srivastava, R. B. (1980) *J. Raman Spectrosc.* **9**, 166–171.
26. Tsubaki, M., Srivastava, R. B. & Yu, N.-T. (1981) *Biochemistry* **20**, 946–952.
27. Petsko, G. A., Saito, M. I. & Yonetani, T. (1978) in *Frontiers of Biological Energetics*, eds. Dutton, P. L., Leigh, J. S. & Scarpa, A. (Academic, New York), Vol. 2, pp. 1011–1016.
28. Nagai, K., Kitagawa, T. & Morimoto, H. (1980) *J. Mol. Biol.* **136**, 271–289.
29. Duff, L. L., Appelman, E. H., Shriver, D. F. & Klotz, I. M. (1979) *Biochem. Biophys. Res. Commun.* **90**, 1098–1103.
30. Phillips, S. E. V. (1980) *J. Mol. Biol.* **142**, 531–554.
31. Yamamoto, H., Kayne, F. J. & Yonetani, T. (1974) *J. Biol. Chem.* **249**, 691–698.
32. Makinen, M. W., Houtchens, R. A. & Caughey, W. S. (1979) *Proc. Natl. Acad. Sci. USA* **76**, 6042–6046.
33. Tucker, P. W., Phillips, S. E. V., Perutz, M. F., Houtchens, R. A. & Caughey, W. S. (1978) *Proc. Natl. Acad. Sci. USA* **75**, 1076–1080.
34. Caughey, W. S., Houtchens, R. A., Lanir, A., Maxwell, J. C. & Charache, S. (1978) in *Biochemical and Clinical Aspects of Hemoglobin Abnormalities*, ed. Caughey, W. S. (Academic, New York), pp. 29–53.
35. Hoffman, B. M., Diemente, D. L. & Basolo, F. (1970) *J. Am. Chem. Soc.* **92**, 61–65.
36. Getz, D., Melemud, E., Silver, B. C. & Dori, Z. (1975) *J. Am. Chem. Soc.* **97**, 3846–3847.
37 Gupta, R. K., Mildvan, A. S., Yonetani, T. & Srivastava, T. S. (1975) *Biochem. Biophys. Res. Commun.* **67**, 1005–1012.
38. Kitagawa, T., Kyogoku, Y., Iizuka, T. & Saito, M. I. (1976) *J. Am. Chem. Soc.* **98**, 5169–5173.
39. Felton, R. H. & Yu, N.-T. (1978) in *The Porphyrins*, ed. Dolphin, D. (Academic, New York), Vol. 3, pp. 347–393.